energies

MDPI

Article

Research on the Thermal Decomposition Characteristics of PE Outer Sheath of High-Voltage Cables Under Different Humidity Levels

Zhaoguo Wu [1], Qian Wang [1], Huixian Huang [2], Yong Li [1], Yulai Kuang [3], Hong Xiang [1], Junwei Liu [4,*] and Zhengqin Cao [4]

[1] State Grid Chongqing Electric Power Research Institute, Chongqing 401123, China; wuzhaoguo@cq.sgcc.com.cn (Z.W.); wangqian@cq.sgcc.com.cn (Q.W.); hvliyong@cq.sgcc.com.cn (Y.L.); xhhyde123@163.com (H.X.)
[2] State Grid Chongqing Electric Power Company, Chongqing 400015, China; huanghuixian@cq.sgcc.com.cn
[3] State Grid Chongqing Electric Power Co. Skill Training Center, Chongqing 401329, China; kuangyulai@cq.sgcc.com.cn
[4] School of Electronic and Electrical Engineering, Chongqing University of Science and Technology, Chongqing 401331, China; caozhengqin@vip.sina.com
* Correspondence: 2023204035@cqust.edu.cn

Abstract

Gas sensors can provide early warning of fires by detecting pyrolysis gas components in the sheaths of high-voltage cables. However, air humidity significantly affects the thermal decomposition gas production characteristics of the outer sheath of high-voltage cables, which in turn affects the accuracy of this warning method. In this paper, the thermal decomposition and gas production characteristics of the polyethylene (PE) outer jacket of high-voltage cables under different air humidities (20–100%) are studied, and the corresponding density functional theory (DFT) simulation calculations are performed using Gaussian 09W software. The results show that with the increase in humidity, the thermal decomposition gas yield of the PE outer jacket of high-voltage cables exhibits a decreasing trend. Under high-humidity conditions (≥68.28%RH), the generation of certain thermal decomposition gases is significantly reduced or even ceases. Meanwhile, the influence of moisture on the thermal decomposition characteristics of PE was analyzed at the micro level through simulation, indicating that the H-free radicals generated by moisture promote the initial decomposition of PE, but the subsequent combination of hydroxyl groups with terminal chain C forms a relatively stable alkoxy structure, increasing the activation energy of the reaction (by up to 44.7 kJ/mol) and thus inhibiting the generation of small-molecule gases. An experimental foundation is laid for the final construction of a fire warning method for high-voltage cables based on the information of thermal decomposition gas of the outer sheath.

Keywords: high-voltage cable; PE outer sheath; humidity; infrared spectroscopy; gas chromatography

check for updates

Academic Editor: Franco Berruti

Received: 25 May 2025
Revised: 29 June 2025
Accepted: 1 July 2025
Published: 4 July 2025

Citation: Wu, Z.; Wang, Q.; Huang, H.; Li, Y.; Kuang, Y.; Xiang, H.; Liu, J.; Cao, Z. Research on the Thermal Decomposition Characteristics of PE Outer Sheath of High-Voltage Cables Under Different Humidity Levels. *Energies* **2025**, *18*, 3537. https://doi.org/10.3390/en18133537

Copyright: © 2025 by the authors. Licensee MDPI, Basel, Switzerland. This article is an open access article distributed under the terms and conditions of the Creative Commons Attribution (CC BY) license (https://creativecommons.org/licenses/by/4.0/).

1. Introduction

With the development of urban construction in China, high-voltage cables are widely used in urban power grids because of their outstanding advantages such as small occupation of ground space, large transmission capacity, high safety, and reliability [1–3]. However, the fire hazards of high-voltage power cables have been increasing in recent

years [4,5]. The causes of cable fire accidents are mostly due to the faults of the cables themselves [6–8]. During the operation of high-voltage power cables, the insulation layer will inevitably be affected by aging and moisture, which in turn leads to the generation of localized discharges, short circuits and other faults [9–11]. When the fault occurs, the cable core conductor may generate a large amount of heat, which finally causes the cable to burn, triggering a major safety accident [12–14]. Before the outer sheath of the cable begins to show open flames, it is often accompanied by the thermal decomposition of the outer sheath. Relevant studies [15–17] indicate that gas components such as Dioctyl Phthalate (DOP) and 2-Ethylhexanol (2-EH), which are significantly related to temperature, are produced during the thermal decomposition process of the outer sheath of high-voltage power cables detected by gas sensors. It can achieve early warning of fires in high-voltage power cables.

In order to investigate the pyrolysis characteristics of high-voltage cable sheath, Kannan P et al. [18] studied the pyrolysis of PE material under different heating rate conditions, and found that the PE material started to decompose obviously from about 400 °C. Jing R et al. [19] studied the pyrolysis characteristics of 110 kV high-voltage cable PVC sheath in air and nitrogen atmosphere, and found that the pyrolysis gases mainly consisted of H_2O and CO_2, in addition to a small amount of alkanes. H_2O and CO_2, in addition to a small number of alkanes. Guo Y et al. [20] conducted thermogravimetric gas chromatography (TGA-GC) experiments and investigated the pyrolysis characteristics of polypropylene cable insulation at 30~600 °C and found that the pyrolysis gases were mainly composed of H_2, CO, C_2H_4 and CH_4. Kajda-Szcześniak M et al. [21] used the coupled TG-MS analysis combined with the TG-FTIR analysis to identify the decomposition mechanisms of waste vinyl panels. Yang S et al. [22] used thermogravimetric-Fourier transform infrared spectroscopy (TG-FTIR) for the pyrolysis of PVC at different oxygen concentrations and found that the oxygen concentration mainly affected the reaction mechanism of the second stage of PVC pyrolysis. Decimus A [23] and other scholars found that by combusting a variety of cables from 0 to 800 °C, PVC cables produced more flammable gases at less than 650 °C; at 800 °C, PVC was observed to release CO. Zheng X [24] and other scholars carried out PVC combustion at 0~600 °C, and found that the PVC heat release rate curve had a maximum peak that could be maintained for a long time. B. Jabłońska et al. [25] used methods such as TG/DTG analysis coupled with FTIR and mass spectroscopy (MS) to analyze the influence of particular components on the pyrolysis process of waste plastics. The authors of [26] reveal that the pyrolysis of PE cable materials occurs predominantly in a single stage, with heating rates affecting the pyrolysis rate. The initial products are mainly alkanes, followed by alkenes and trace alkynes. Stanislav Honus et al. [27] detected that at 500 °C, alkanes account for 36.07% of the pyrolysis gases, predominantly methane (propane only 9.91%), while at 700 °C, substantial hydrogen is generated due to the conversion of alkenes and alkynes. However, domestic and foreign scholars' studies on the pyrolysis/combustion behavior of cable sheath-related polymers mainly focus on the whole process of overheating decomposition of cable sheath-related polymers. This study focuses on early-warning research for high-voltage cable fires, specifically targeting the pre-ignition and pre-flaming stages. As reported in Reference [28], the ignition point of PE is 350 °C. By integrating the maximum operating temperature for cable conductor short-circuits specified in China's national standard GB/T 11017.1-2024 [29], a target temperature of 250 °C was selected to investigate the thermal decomposition gas generation characteristics of PE outer sheaths, providing a scientific basis for early cable fault warning.

Related studies have shown that air humidity can promote or inhibit the pyrolysis process, thus affecting the yield of pyrolysis products [30,31]. At present, there is a lack of systematic research on the characteristics of humidity and thermal decomposition gas

production of cable sheaths. According to the information of China Meteorological Network, excluding the extreme climate, the average relative humidity in the cities of China is around 20~80% [32]. To this end, this study intends to carry out thermal decomposition tests and Gaussian calculations with relative humidity of 25%, 40%, 55%, 65%, 75%, and 95%. It is the first to propose considering the influence of different humidity environments on the thermal decomposition of the PE outer sheath of high-voltage cables, in order to more truly reflect the early overheating faults of high-voltage cables under different regions and working conditions and to obtain the gas generation characteristics of the thermal decomposition of the PE outer sheath at the experimental and simulation levels.

2. Thermal Decomposition Test Method

This study was carried out on a self-built thermal decomposition test platform for high-voltage cable PE outer sheath, as shown in Figure 1. The test platform is mainly composed of three parts: temperature control, humidity control, and gas detection.

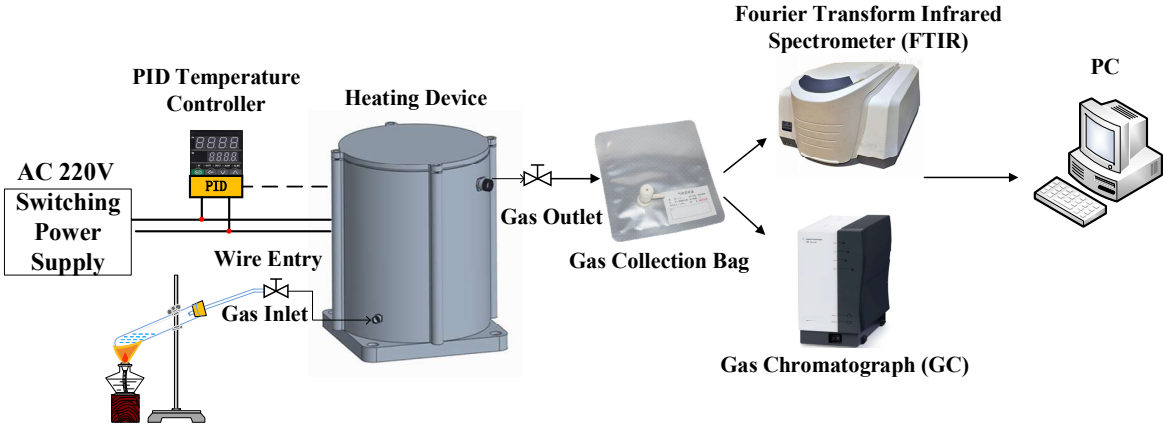


Figure 1. Thermal decomposition experiment platform for high-voltage power cable outer sheath.

The PE outer jacket of the high-voltage cable used in this study is YJLW03-64/110 kV, with the structure standard referring to IEC 60229:2007 [33] and the Chinese national standard GB/T 11017.2-2014 [34]. The thickness of the PE outer sheath used in this paper is approximately 4 mm, and the mass of the PE sample used in each experiment is 50 ± 0.1 g. The heating device is a stainless steel cylindrical tank with a volume of approximately 10 L. The infrared spectroscopy model is the FTIR-850 Fourier Transform Infrared Spectrometer (FTIR-850) of Tianjin GD, which utilizes a high sensitivity DLATGS detector. The gas chromatography model is Agilent 490, which adopts modular design and supports multi-detector adaptation, such as FID and TCD.

Before starting the test, the interior of the heating chamber was scrubbed and purged to ensure that the interior of the chamber was dry. According to the relative humidity formula (Equation (1)), a fixed mass of H_2O was weighed and added into the vacuum test tube, which was heated to fully vaporize the H_2O and passed into the vacuum heating device. Subsequently, dry air was charged until the air pressure in the airtight chamber reached 1 atm. Then, it was left to stand for 30 min so that the dry air and H_2O were fully mixed homogeneously in the heating device. After that, the temperature of the local heat source was adjusted to 250 °C, and the test was started, which lasted for 120 min, and the sample gas in the heating chamber was collected from the air outlet at the end of the test. After the collection was completed, we removed the sample and cleaned the heating chamber, and, again, pumped the heating chamber to a vacuum state, in preparation for the next test. The collected gases were detected by gas chromatography for the thermal decomposition products, and the collected gases were quantitatively analyzed by external

standard method. Through the preparation of a known concentration of standard gases (containing CO, CO_2, C_2H_2, and other target components), we aimed to establish a linear relationship between the chromatographic peak area and the concentration, and then, based on the peak area of the sample, achieve quantitative analysis. The operation followed the Chinese national standard GB/T 13610-2020 [35] and other gas chromatography external standards:

$$\varphi = \frac{\rho_v}{\rho_s} \quad (1)$$

where φ is relative humidity, ρ_v is actual absolute humidity and ρ_s is saturated absolute humidity.

3. Results and Discussion

3.1. Infrared Spectroscopy Test Results and Analysis

After the microhydrometer detection, the actual relative humidity at the time of the test was 24.58% RH, 41.02% RH, 54.68% RH, 67.53% RH, 78.98% RH, 99.54% RH. Figure 2 shows the infrared spectra of the thermal decomposition products of the outer jacket of high-voltage cables under different humidity levels.

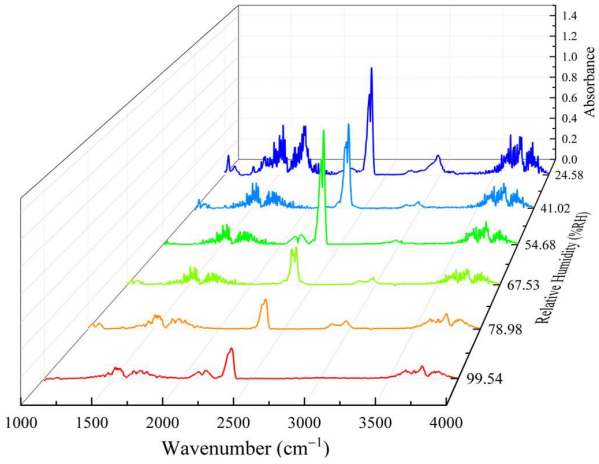


Figure 2. Infrared spectra of thermal decomposition products of PE outer sheath of high-voltage cables at different humidity levels.

As can be seen from Figure 2, the overall absorbance of the infrared spectra of the thermal decomposition gas products of the outer sheath of the high-voltage cable shows a decreasing trend with an increase in the ambient humidity. This means that the generation of thermal decomposition gas shows a decreasing trend with an increase in ambient humidity. Among them, the highest absorbance of thermal decomposition products was observed at an ambient humidity of 24.58% RH. The antisymmetric deformation vibration of =C–H functional group was generated near the wave number 1000 cm^{-1}, the telescopic vibration of =C–H occurred near the wave number 3020–3080 cm^{-1}, and the –C=C– stretching vibration. The vibrational mode of these functional groups indicates that the resultant product may be an olefinic gas [36]. An antisymmetric deformation vibration of the –CH_3 functional group was produced near the wave number 1460 cm^{-1}. A shear vibration of the –CH_2– functional group occurred near the wave number 1350–1470 cm^{-1}, as well as a stretching vibration of –CH_2–, so the vibration of these functional groups may be the generation of alkane gas [37]. The telescopic motion of ≡C–H functional group occurred near the wave number 3270–3300 cm^{-1}, which indicated the generation of alkyne gases from the thermal decomposition products. While carbon dioxide gas was generated at wave number 2349 cm^{-1}, water vapor was generated around wave numbers 1300–2000 cm^{-1} and 3500–3950 cm^{-1} [38]. As the humidity rose, the

absorbance of the thermal decomposition gas infrared spectrogram gradually decreased, but the infrared absorption peaks of some of the characteristic gases can still be detected. In addition, it is worth noting that at the maximum humidity of 99.54% RH, no functional group vibration was found near 2500–3500 cm^{-1}, which indicates that the –CH_2– stretching vibration near 2850–2960 cm^{-1} and the ≡C–H functional group stretching motions were not occurring.

3.2. Gas Chromatography Test Results and Analysis

After the gas chromatography test, seven kinds of thermal decomposition products were identified from the PE outer sheath of high-voltage cables under different humidity conditions, and the amounts of these products are shown in Figure 3. CO_2 production was 16,012 μL/L at 27.38% RH but only 4882 μL/L at 99.76% RH, which is a more than threefold difference in concentration. The generation of C_2H_2 was 9691 μL/L at 27.38% RH and 3874 μL/L at 99.76% RH; the generation of C_2H_2 at low humidity was almost three times higher than that at high humidity; the generation of C_2H_4 and CO gases at different humidities was similar, and the generation of C_2H_4 was 582 μL/L at low to high humidity. These were 582 μL/L, 428 μL/L, 349 μL/L, 252 μL/L, 188 μL/L, and 165 μL/L, while the generation of CO was 651 μL/L, 472 μL/L, 383 μL/L, 256 μL/L, 188 μL/L, and 173 μL/L from low to high humidity, and the generation of both gases was inversely proportional to the humidity increase. The generation of C_2H_6, C_3H_6, and C_3H_8 gases at 250 °C was not much, and at high humidity, the generation was even less; the generation of C_2H_6 and C_3H_6 gases at 99.76% RH was only 1 μL/L and 2 μL/L, respectively, and the generation of C_3H_8 gas at 55.13% RH was detected as 1 μL/L, which is the highest among the two gases in the world. We detected 1 μL/L at 55.13% RH, while C_3H_8 gas was already detected at 1 μL/L at 68.28% RH, and the generation of C_3H_8 gas was no longer detected.

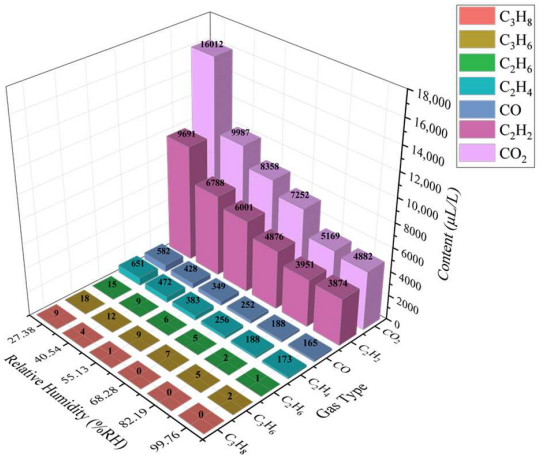


Figure 3. Composition and yields of thermal decomposition products from high-voltage cable PE outer sheath at different humidity levels.

The gas chromatography test results show that high-voltage cable PE outer sheath thermal decomposition gas generation with humidity has a downward trend, and the high-humidity environment reduces the generation of thermal decomposition gas. The variation in CO generation with humidity is shown in Figure 4a: at low humidity, CO production decreases rapidly with increasing humidity, while at high humidity, the decline tends to stabilize, presenting an overall exponential downward trend. Similarly, the variation in CO_2 generation in Figure 4b follows an exponential decrease pattern similar to that of CO, probably due to the fact that the generation of CO and CO_2 is greatly affected by humidity but the decline magnitude is significantly greater.

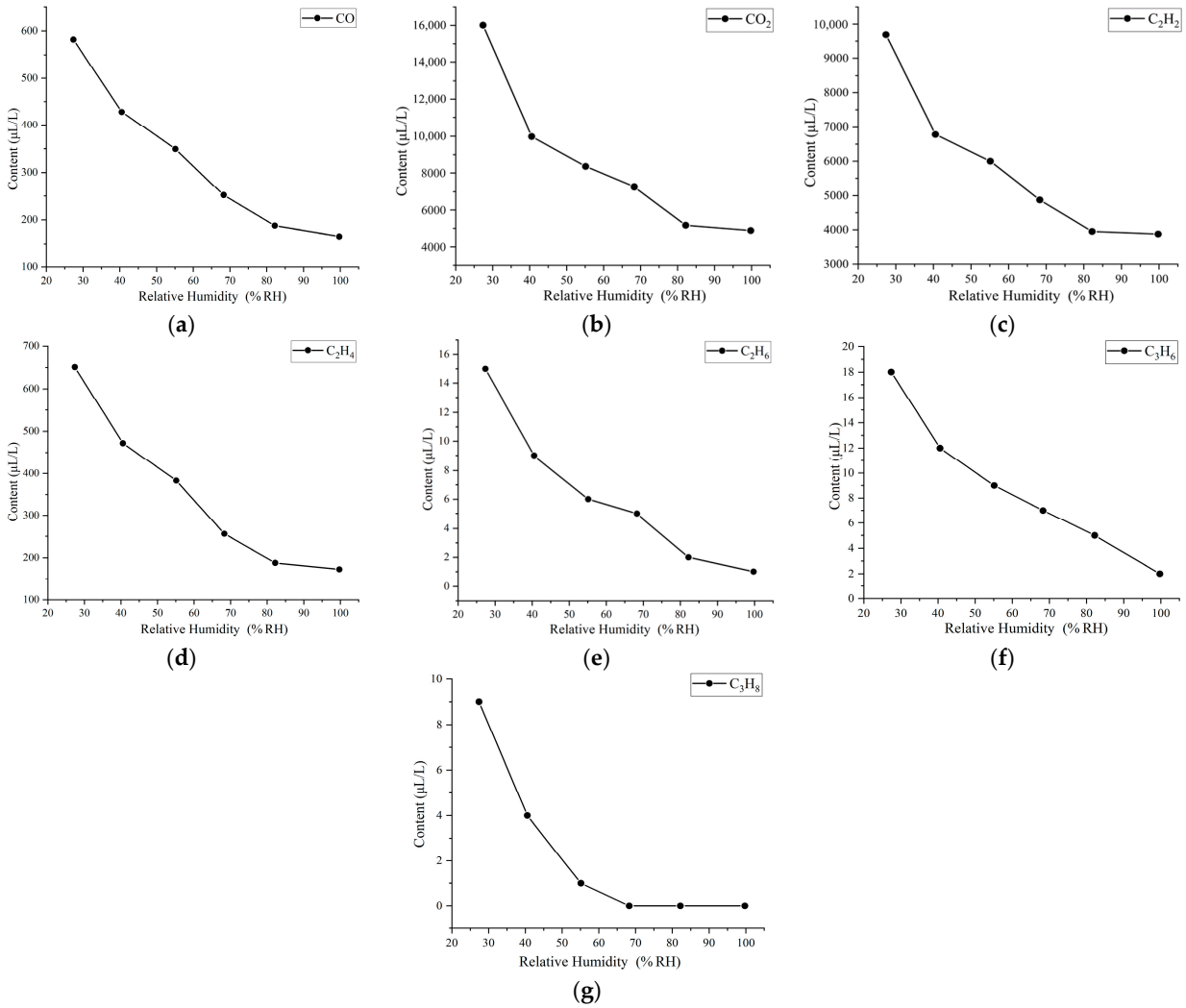


Figure 4. Variations in individual thermal decomposition gases from high-voltage cable PE outer sheath at different humidity levels: (**a**) CO, (**b**) CO_2, (**c**) C_2H_2, (**d**) C_2H_4, (**e**) C_2H_6, (**f**) C_3H_6, and (**g**) C_3H_8.

The variation patterns of C_2H_2 and C_2H_4 production with humidity increase are shown in Figures 4c and Figure 4d, respectively. Both of them showed an exponential decreasing trend, and the decreasing rate of C_2H_2 was significantly higher than that of C_2H_4. When the humidity increased from 27.38% RH to 99.76% RH, the concentration of C_2H_2 decreased from 9691 μL/L to 3874 μL/L (59% decrease), while that of C_2H_4 decreased from 582 μL/L to 165 μL/L (72% decrease). The concentrations of C_2H_6 and C_3H_4 showed a nearly straight-line decreasing tendency with the increase in humidity, as shown in Figure 4e,f. The concentrations of both were only 1 μL/L and 2 μL/L at high humidity (99.76% RH). It is noteworthy that C_3H_8 was completely undetected at humidity $\geq$ 68.28% RH, as shown in Figure 4g. Compared with the existing studies, this experiment quantified, for the first time, the differential inhibition effect of humidity on PE pyrolysis gas. Compared with a previous study on PVC sheath by Jing R et al. [19], the sensitivity of PE sheath pyrolysis gases to humidity was higher, especially the zero generation of C_3H_8 at 68.28% RH, which provides a key threshold for the establishment of the humidity compensation model in cable fire warning.

Figure 5 shows a comparative chart of the changes in the generation patterns of thermal decomposition products for high-voltage PE outer sheaths under different humidity conditions. It can be seen that the concentrations of the seven gases detected by gas

chromatography all showed a downward trend with the increase in humidity. Among them, CO_2 and C_2H_2 had the fastest decreasing rate, CO and C_2H_4 had the second decreasing rate after the first two, and C_3H_6, C_2H_6, and C_3H_8 had the slowest decreasing rate. At high humidity, only trace amounts of C_3H_6 and C_2H_6 gases were generated (or even not generated), and C_3H_8 gas was not even generated at high humidity.

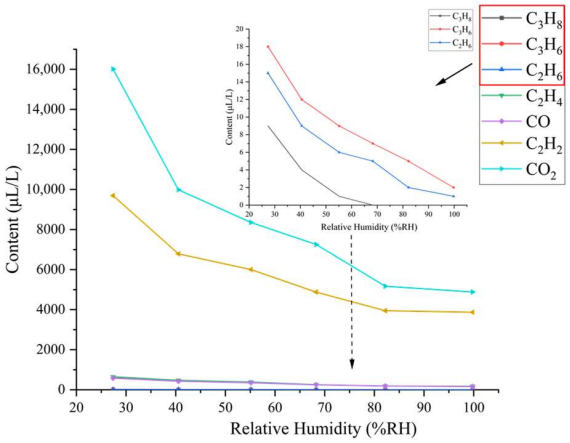


Figure 5. Comparison of the variations in the generation of thermal decomposition products from high-voltage PE outer sheaths at different humidity levels.

3.3. Gaussian Simulation Calculation Analysis

Pure PE consists of long-chain alkanes (–CH_2–CH_2–) n. The actual structure of PE outer sheath is complex and variable, so the study of PE thermal decomposition often relies on low-molecular-mass model compounds. These model compounds share a similar chemical structure with real PE (e.g., long-chain alkanes with ≥95% (–CH_2–CH_2–) repeat units in PE sheaths), leading to similar thermal decomposition mechanisms and intermediate product (e.g., C_2H_4, C_3H_6) distributions [39]. Using Gaussian 09W software, we optimized the structures of reactants, intermediates, transition states, and products via density functional theory (DFT) with the B3LYP functional and 6-311++G(d, P) basis set. In this study, an isotactic PE model with a degree of polymerization of 10 was employed. Although this model cannot fully simulate long-chain effects, it captures key features such as chain-end active sites and C–C bond dissociation energy differences and significantly reduces the computational complexity of quantum chemical calculations while avoiding the exponential growth of degrees of freedom.

As shown in Figure 6, due to the symmetry of the PE model compound, the C(1)–C(2) and C(9)–C(10) bond dissociation energies are equal to 340.13 kJ/mol and the C(2)–C(3) and C(8)–C(9) bonds. The dissociation energies of C(3)–C(4) and C(7)–C(8) bonds are equal to 332.05 kJ/mol; C(4)–C(5) and C(6)–C(7) bonds are equal to 331.34 kJ/mol; C(4)–C(5) and C(6) –C(7) bonds are equal to 331.34 kJ/mol; C(4)–C(5) and C(6)–C(7) bonds are equal to 331.34 kJ/mol; and C(4)–C(5) and C(6)–C(7) bonds are equal to 331.34 kJ/mol. C(4)–C(5) and C(6)–C(7) bond dissociation energy is 331.34 kJ/mol; the C(5)–C(6) bond dissociation energy is the smallest, 326.24 kJ/mol; the C–H bond dissociation energy is the largest, 442.14 kJ/mol, as the magnitude of bond ionization energy directly characterizes the energy threshold for chemical bond breaking. Therefore, during the thermal decomposition reaction of PE, the C–C bond is easier to break and the C(5)–C(6) bond is most likely to break first. According to experiments and related studies, the thermal decomposition of PE mainly occurs random cracking [40,41], and the main product is C_2H_4. Based on this, three thermal decomposition reaction paths of PE were designed to analyze the effect of

air humidity on the thermal decomposition of high-voltage cable outer sheaths from a microscopic point of view.

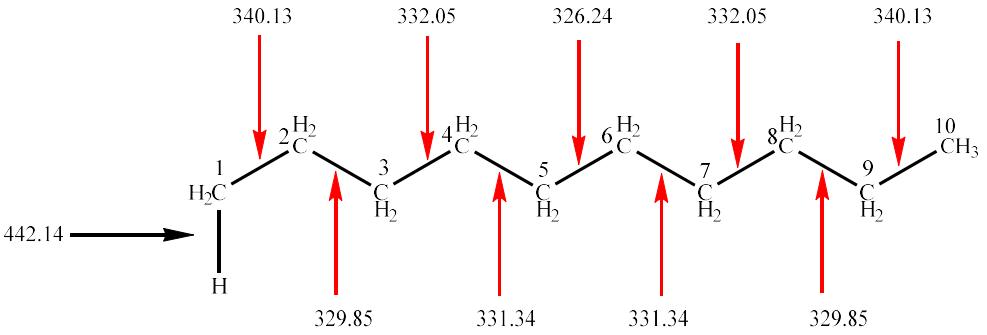


Figure 6. Structural formulae and bonding energies of major bonds of isotactic PE model compounds (unit: kJ/mol).

As shown in Figures 7 and 8, in reaction path 1, model compound **1** can pass through transition state TS1 to form intermediate products 2 (pentane, C_5H_{12}) and 3 (1-pentene, C_5H_{10}), which has a reaction energy barrier of 345.6 kJ/mol and absorbs 6.7 kJ/mol of energy. Intermediate 2 undergoes further reaction via transition state TS2 to form intermediate 4 (ethane, C_3H_8) and ethylene, which has a reaction energy barrier of 533.8 kJ/mol and absorbs 139.7 kJ/mol of energy. Intermediate product 4 was further reacted via transition state TS3 to give methane 5 and ethylene with a reaction energy barrier of 465.8 kJ/mol and absorption of 39.7 kJ/mol.

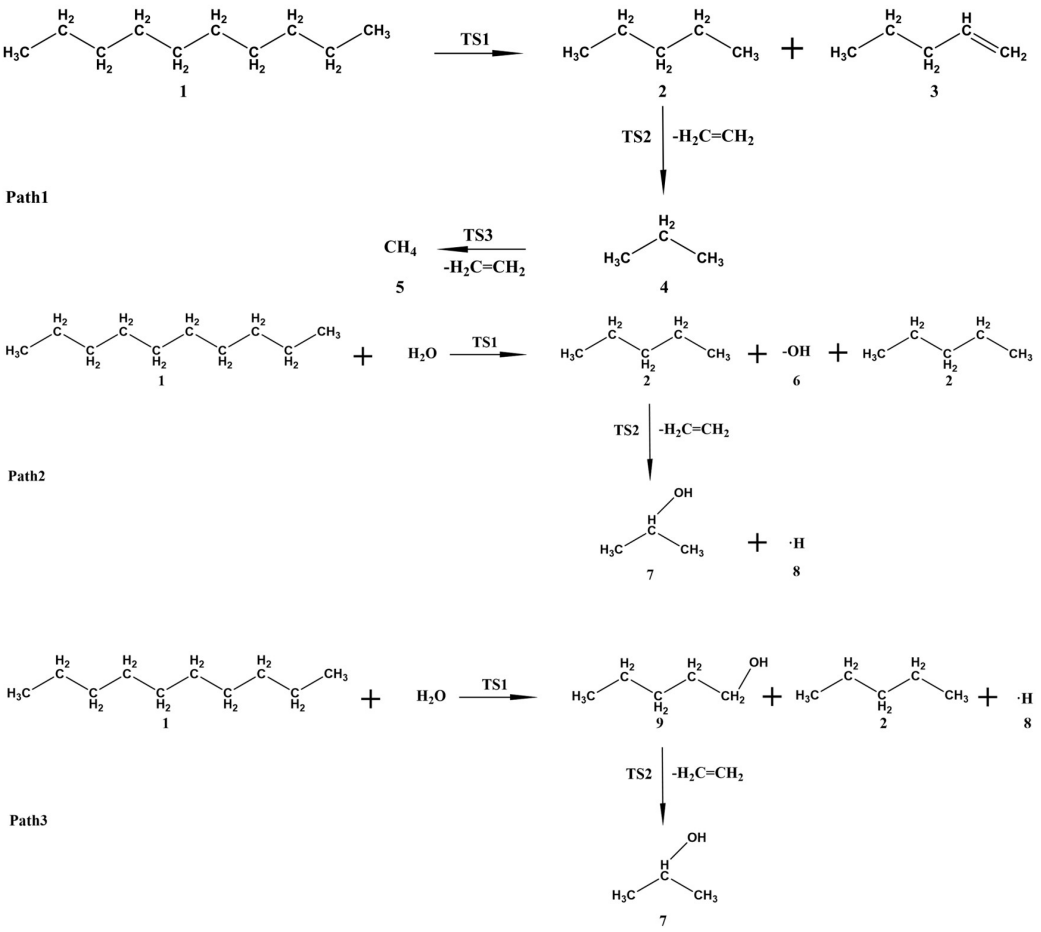
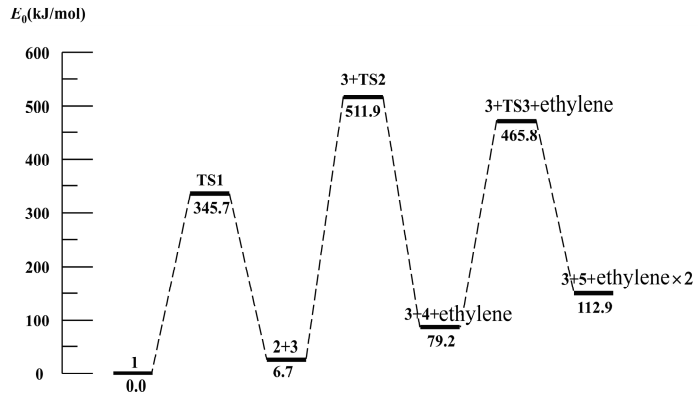
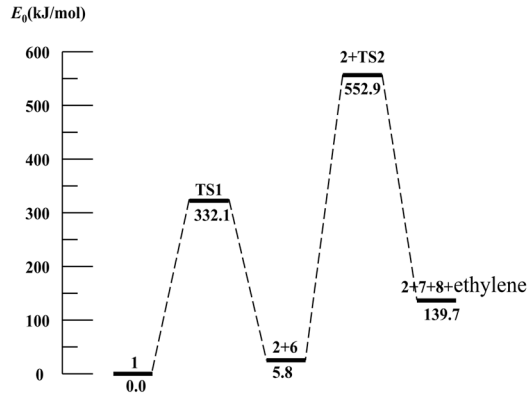


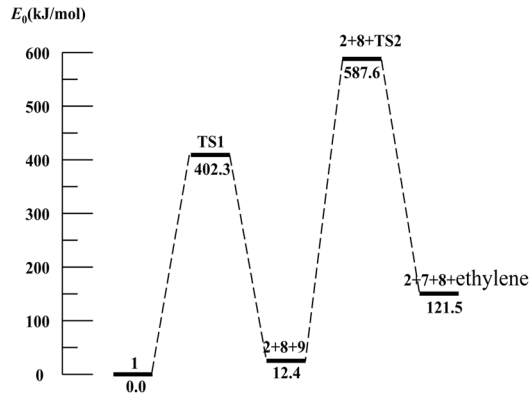
Figure 7. Thermal decomposition pathways of PE.



(**a**) path 1



(**b**) path 2



(**c**) path 3

Figure 8. Energy barrier diagram of thermal decomposition reactions.

Compared with path 1, in reaction path 2, the water molecules attack the model compound **1** scaffold, and the hydrogen radicals detached by water molecules combine with the C atoms at the chain ends to form intermediate product 2 and hydroxyl group 6 via transition state TS1, with a reaction energy barrier of 332.1 kJ/mol and absorption of 5.8 kJ/mol energy, which is 23.5 kJ/mol lower than that of path 1. This suggests that in the early stage of PE thermal decomposition, the H_2O can promote C–C bond breaking. Intermediate product 2 and hydroxyl 6 via, transition state TS2 further reaction to form intermediate products 7 (2-propanol, C_3H_8O), 8 (hydroxyl radical) and ethylene, the reaction energy barrier of 552.9 kJ/mol, absorbing 133.9 kJ/mol of energy, which is 19.1 kJ/mol

higher than that of path 1, and with hydroxyl and end-chain C atoms combining to form a more stable alkoxy structure. Compared to path 1, path 2 requires higher activation energy to form small molecule products via the transition state TS2, which is difficult to further decompose after generating the intermediate product 7.

In reaction path 3, water molecules attack the model compound 1 scaffold, and the hydroxyl group detached by the water molecules combines with the end-chain C atoms to form a more stable alkoxyl structure, and intermediate products 2, 8, and 9 (1-pentanol, $C_5H_{12}O$) are formed via the transition state TS1, which has a reaction energy barrier of 402.3 kJ/mol and absorbs 12.4 kJ/mol of energy, and the activation energy required for the breakage of the C–C bond increases by 56.7 kJ/mol compared with that of path 1. The alkoxy structure-containing intermediate 9 undergoes further reaction to form intermediate 7 and ethylene via transition state TS2, with a reaction energy barrier of 587.6 kJ/mol, which is an increase of 44.7 kJ/mol compared to path 2.

According to the calculation results, PE decreases the reaction energy barrier during thermal decomposition due to H radicals generated from the thermal decomposition of H_2O, which promotes the initial decomposition of PE. However, during further thermal decomposition, the hydroxyl radicals produced by the thermal decomposition of water molecules combined with the end-chain C to form an alkoxy structure will increase the subsequent reaction energy barrier unfavorable to the generation of other small molecule gases, which may be one of the reasons for the decrease in gas production after the increase in humidity.

4. Conclusions

In this study, the thermal decomposition of high-voltage cables was carried out on a platform built by ourselves, and the thermal decomposition characteristics of PE outer sheath of high-voltage cable were studied under different humidity levels. The main conclusions are as follows:

(1) Environmental humidity significantly influences the thermal decomposition process of high-voltage cable PE outer sheaths. With increasing humidity, the gas evolution during PE outer sheath thermal decomposition exhibits a downward trend. When humidity exceeds 68.28%RH, the generation of certain pyrolysis gases (e.g., C_3H_6) becomes extremely low, even below the detection limit of gas chromatography and thus undetected.

(2) From the micro-level analysis via Gaussian 09W calculations, it can be seen that during PE thermal decomposition, the decomposition of water molecules into H radicals promotes the initial decomposition of PE. However, the resulting hydroxyl groups combine with end-chain carbon to form an alkoxyl structure, which increases the subsequent reaction barriers and inhibits the generation of other small-molecule gases, leading to a reduction in gas production.

Currently, the study only focuses on PE sheath materials and has investigated the pyrolysis gas evolution characteristics under six different humidity levels ranging from 20% to 100%. In the next step, the humidity gradient will be refined to systematically explore the pyrolysis gas characteristics of different sheath materials (e.g., PVC), aging degrees, and oxygen concentrations. Based on the quantitative relationships obtained in this study, a humidity-compensated cable fire warning model will be constructed, and its reliability will be verified through simulated tests in actual cable tunnel environments, providing more comprehensive theoretical support for engineering applications.

Author Contributions: Investigation, H.H.; methodology, Z.W.; project administration, J.L.; resources, Y.K.; software, Q.W. and Y.L.; supervision, J.L.; validation, Z.W., Q.W. and J.L.; visualization, Q.W.; writing—original draft, Z.W., Q.W. and H.X.; writing—review and editing, H.H., Y.K. and Z.C. All authors have read and agreed to the published version of the manuscript.

Funding: This research was funded by the State Grid Chongqing Electric Power Company Science and Technology Project (2024 Yudian Technology 12#).

Data Availability Statement: The original contributions presented in this study are included in the article material. Further inquiries can be directed to the corresponding author.

Conflicts of Interest: Authors Huixian Huang and Yulai Kuang were employed by the company State Grid Chongqing Electric Power Company. The remaining authors declare that the research was conducted in the absence of any commercial or financial relationships that could be construed as a potential conflict of interest.

References

1. Yuan, J.; Ouyang, B.; Xia, R.; Wang, G.; Liu, S. Research on the effectiveness evaluation method of on-line partial discharge monitoring device for high-voltage cables and field application. *High Volt. Eng.* **2023**, *49*, 17–23. [CrossRef]
2. Wang, T.; Tan, L.; Xie, S.; Ma, B. Development and applications of common utility tunnels in China. *Tunn. Undergr. Space Technol.* **2018**, *76*, 92–106. [CrossRef]
3. Pan, R.; Zhu, G.; Xu, G.; Liu, X. Experimental analysis on burning rate and temperature profile produced by pool fire in a curved tunnel as a function of fire location. *Process Saf. Environ. Prot.* **2021**, *152*, 549–567. [CrossRef]
4. National Fire and Rescue Administration. *China Fire Yearbook 2018 Edition*; Yunnan People's Publishing House: Kunming, China, 2018.
5. Guo, W.; Pu, Z.; Ren, Z.; Zhou, S.; Quan, L.; Men, Y.; Pan, Z. Analysis of abnormal detection data of fire accident in power cable tunnel and field test study on characteristic parameters of tunnel fire. *Front. Energy Res.* **2022**, *10*, 860707. [CrossRef]
6. Wang, Y.; Kang, N.; Lin, J.; Lua, S.; Liew, K.M. On the pyrolysis characteristic parameters of four flame-retardant classes of PVC sheathless cable insulation materials. *J. Anal. Appl. Pyrolysis* **2023**, *170*, 105901. [CrossRef]
7. Zhou, J.; Liu, G.; Wang, S.; Zhang, H.; Xu, F. TG-FTIR and Py-GC/MS study of the pyrolysis mechanism and composition of volatiles from flash pyrolysis of PVC. *J. Energy Inst.* **2020**, *93*, 2362–2370. [CrossRef]
8. Courty, L.; Garo, J.P. External heating of electrical cables and auto-ignition investigation. *J. Hazard. Mater.* **2017**, *321*, 528–536. [CrossRef]
9. Liu, J.; Ouyang, B.; Xia, R.; Fei, W. Assessment of the insulation aging state of high voltage XLPE cables. *Electr. Power Eng. Technol.* **2021**, *40*, 141–149. [CrossRef]
10. Duan, Y.; Han, M.; Lan, R.; Li, G.; Wang, Z. Insulation Characteristics and Failure Mechanism of High-Voltage Cables under Different Thermal Aging Temperatures. *Trans. China Electrotech. Soc.* **2024**, *39*, 45–54. [CrossRef]
11. Lee, H.G.; Jung, J.S.; Kim, J.G. Measurement of activation energy and accelerated degradation time by thermal analysis methods for polymeric insulating materials. *J. Electr. Eng. Technol.* **2021**, *16*, 515–524. [CrossRef]
12. Xu, D.; Li, Y.; Yang, X.; Zhong, H.; Li, J.; Li, J.; Huang, Y. Enhancing resilience in urban utility tunnels power transmission systems: Analysing temperature distribution in near-wall cable fires for risk mitigation. *Tunn. Undergr. Space Technol.* **2024**, *152*, 105911. [CrossRef]
13. Zhang, J.; Huang, Y.; Qiu, X.; Zhu, T. A review on fire research of electric power grids of China: State-of-the-art and new insights. *Fire Technol.* **2024**, *60*, 1027–1076. [CrossRef]
14. Huo, Y.; Xu, X.; Li, Y.; Li, R.; Yu, Z.; Wang, W. Experimental and theoretical research on the temperature evolution law of overcurrent fault wires. *Fire Mater.* **2024**, *48*, 632–641. [CrossRef]
15. Liu, Y.; Geyik, U.; Kobald, A.; Yang, A.; Wang, X.; Weimar, U.; Rong, M.; Bârsan, N. Overheat diagnosis of power cable based on gas sensors: Device/material exploration. *Sens. Actuators B Chem.* **2022**, *350*, 130837. [CrossRef]
16. Lei, F.; Chu, J.; Liu, Y.; Yang, A.; Yuan, H.; Wang, X.; Rong, M. Fault diagnosis of cable overheating based on semiconductor gas sensing array. *Trans. China Electrotech. Soc.* **2023**, *38*, 3651–3664. [CrossRef]
17. Yi, J.; Chen, W.; Han, J.; Chen, D. Sensitive and selective detection of plasticizer vapors with modified-SnO2 hollow nanofibers for electrical fire warning. *Sens. Actuators B Chem.* **2019**, *287*, 364–370. [CrossRef]
18. Kannan, P.; Ibrahim, S.; Reddy, K.S.K.; Al Shoaibi, A.; Srinivasakannan, C. A comparative analysis of the kinetic experiments in polyethylene pyrolysis. *J. Energy Resour. Technol.* **2014**, *136*, 024001. [CrossRef]
19. Jing, R.; Wei, G.; Du, K.; Cao, Z.; Yan, H. Experimental Study on Thermal Decomposition of Polyvinyl Chloride Outer Sheath of 110 kV High Voltage Cable. *J. Electr. Eng. Technol.* **2025**, *20*, 861–872. [CrossRef]
20. Guo, Y.; Wu, Y.; Zhang, D.; Fang, R.; Zhang, X. Revealing the pyrolysis mechanism of polypropylene cable insulation: A combined study of TG-GC experiments and RMD/DFT simulations. *J. Appl. Polym. Sci.* **2024**, *141*, e55245. [CrossRef]
21. Kajda-Szcześniak, M.; Czop, M. Comparison of Pyrolysis and Combustion Processes of Vinyl Floor Panels Using Thermogravimetric Analysis (TG-FTIR) in Terms of the Circular Economy. *Energies* **2022**, *15*, 1516. [CrossRef]

22. Yang, S.; Wang, Y.; Man, P. Kinetic Analysis of Thermal Decomposition of Polyvinyl Chloride at Various Oxygen Concentrations. *Fire* **2023**, *6*, 404. [CrossRef]
23. Decimus, A.; Sonnier, R.; Zavaleta, P.; Suard, S.; Ferry, L. Study of gases released under incomplete combustion using PCFC–FTIR. *J. Therm. Anal. Calorim.* **2019**, *138*, 753–763. [CrossRef]
24. Zheng, X.; Cai, G.; Guo, J.; Gao, W.; Huang, Y.; Tong, X. Combustion characteristics and thermal decomposition mechanism of the flame-retardant cable in urban utility tunnel. *Case Stud. Therm. Eng.* **2023**, *44*, 102887. [CrossRef]
25. Jabłońska, B.; Poznańska, G.; Jabłoński, P.; Zwolińska, J. Thermochemical Valorization of Plastic Waste Containing Low Density Polyethylene, Polyvinyl Chloride and Polyvinyl Butyral into Thermal and Fuel Energy. *Energies* **2024**, *17*, 3458. [CrossRef]
26. Wu, J.; Chen, T.; Luo, X.; Han, D.; Wang, Z.; Wu, J. TG/FTIR analysis on co-pyrolysis behavior of PE, PVC and PS. *Waste Manag.* **2014**, *34*, 676–682. [CrossRef]
27. Honus, S.; Kumagai, S.; Fedorko, G.; Molnár, V.; Yoshioka, T. Pyrolysis gases produced from individual and mixed PE, PP, PS, PVC, and PET-Part I: Production and physical properties. *Fuel* **2018**, *221*, 346–360. [CrossRef]
28. Lv, L.; Duan, C.; Ji, S.; Rao, Z.; Xu, M.; Lin, Z. Overview of ignition mechanism and combustion characteristic of wire and cable. *High Volt. Eng.* **2022**, *48*, 612–625. [CrossRef]
29. *GB/T 11017.1-2024*; Power Cables with Cross-Linked Polyethylene Insulation and Their Accessories for Rated Voltage of 66 kV (Um = 72.5 kV)and 110 kV(Um = 126 kV)—Part 1: Test Methods and Requirements. Standards Press of China: Beijing, China, 2024.
30. Wang, S. Research on the influence of air humidity on coal spontaneous combustion characteristics and oxidation kinetics parameters. *Safe. Coal Min.* **2024**, *55*, 98–105. [CrossRef]
31. Lai, Y.; Liu, X.; Davies, M.; Fisk, C.; Holliday, M.; King, D.; Zhang, Y.; Willmott, J. Characterisation of wood combustion and emission under varying moisture contents using multiple imaging techniques. *Fuel* **2024**, *373*, 132397. [CrossRef]
32. Zhang, H.; Yoshino, H. Analysis of indoor humidity environment in Chinese residential buildings. *Build. Environ.* **2010**, *45*, 2132–2140. [CrossRef]
33. *IEC 60229:2007*; Electric Cables—Tests on Extruded Oversheaths with a Special Protective Function. International Electrotech-nical Commission: Geneva, Switzerland, 2007.
34. *GB/T 11017.2-2014*; Power Cables with Cross-Linked Polyethylene Insulation and Their Accessories for Rated Voltage of 110 kV (Um = 126 kV)—Part 2: Power Cables. Standards Press of China: Beijing, China, 2024.
35. *GB/T 13610-2020*; Analysis of Natural Gas Composition—Gas Chromatography. Standards Press of China: Beijing, China, 2020.
36. Jameel, A.G.A.; Han, Y.; Brignoli, O.; Telalović, S.; Elbaz, A.M.; Im, H.G.; Roberts, W.L.; Sarathy, S.M. Heavy fuel oil pyrolysis and combustion: Kinetics and evolved gases investigated by TGA-FTIR. *J. Anal. Appl. Pyrolysis* **2017**, *127*, 183–195. [CrossRef]
37. Li, X.; Zhang, J.; Yang, X.; Jin, Y.; Lv, Z.; Lan, S.; Zhu, D.; Dang, L. Self-emulsification synthesis of epoxy phosphate ester and its flame-retardant mechanism in flexible poly (vinyl chloride)/magnesium hydroxide composites. *J. Appl. Polym. Sci.* **2024**, *141*, e55354. [CrossRef]
38. Yang, J.; Chen, H.; Zhao, W.; Zhou, J. TG–FTIR-MS study of pyrolysis products evolving from peat. *J. Anal. Appl. Pyrolysis* **2016**, *117*, 296–309. [CrossRef]
39. Tian, Z.; Liu, W.; Yu, Q.; Ji, W. Pyrolysis and carbonization of polyvinyl chloride under electric field: A computational study. *Chem. Phys. Lett.* **2021**, *770*, 138450. [CrossRef]
40. Bockhorn, H.; Hornung, A.; Hornung, U. Mechanisms and kinetics of thermal decomposition of plastics from isothermal and dynamic measurements. *J. Anal. Appl. Pyrolysis* **1999**, *50*, 77–101. [CrossRef]
41. Luo, H.; Zhao, Y.; Li, Y.; Xiang, Y.; He, D.; Pan, X. Aging of microplastics affects their surface properties, thermal decomposition, additives leaching and interactions in simulated fluids. *Sci. Total Environ.* **2020**, *714*, 136862. [CrossRef]

Disclaimer/Publisher's Note: The statements, opinions and data contained in all publications are solely those of the individual author(s) and contributor(s) and not of MDPI and/or the editor(s). MDPI and/or the editor(s) disclaim responsibility for any injury to people or property resulting from any ideas, methods, instructions or products referred to in the content.